Delft University of Technology

The effect of riboflavin on the microbiologically influenced corrosion of pure iron by Shewanella oneidensis MR-1

Chang, Weiwei; Li, Yangyang; Li, Ziyu; Lou, Yuntian; Cui, Tianyu; Qian, Hongchang; Mol, Arjan; Zhang, Dawei

Important note
To cite this publication, please use the final published version (if applicable).
Please check the document version above.

The effect of riboflavin on the microbiologically influenced corrosion of pure iron by *Shewanella oneidensis* MR-1

Weiwei Chang [a,b,1], Yangyang Li [b,1], Ziyu Li [c], Yuntian Lou [a,b], Tianyu Cui [a,b], Hongchang Qian [a,b,d], Arjan Mol [c], Dawei Zhang [a,b,d,*]

[a] *Beijing Advanced Innovation Center for Materials Genome Engineering, Institute for Advanced Materials and Technology, University of Science and Technology Beijing, Beijing 100083, China*
[b] *National Materials Corrosion and Protection Data Center, University of Science and Technology Beijing, Beijing 100083, China*
[c] *Delft University of Technology, Department of Materials Science and Engineering, Mekelweg 2, Delft 2628CD, The Netherlands*
[d] *BRI Southeast Asia Network for Corrosion and Protection (MOE), Shunde Graduate School of University of Science and Technology Beijing, Foshan 528399 China*

ABSTRACT

The microbiologically influenced corrosion of pure iron was investigated in the presence of *Shewanella oneidensis* MR-1 with various levels of exogenous riboflavin (RF) serving as electron shuttles for extracellular electron transfer (EET). With more RF available, a larger and denser phosphate layer was formed on the surface of pure iron by the bacteria. The results of electrochemical impedance spectroscopy, linear polarization resistance and potentiodynamic polarization tests showed that the product layer provided good corrosion protection to the pure iron. Using electrochemical noise, we observed that the addition of RF accelerated the corrosion at the initial stage of immersion, thereby accelerating the deposition of products to form a protective layer subsequently.

1. Introduction

Microbiologically influenced corrosion (MIC) is regarded as one of the important reasons for accelerating metals degradation and has a significant detrimental impact in a wide range of industries [1–4]. Several typical mechanisms of MIC have been extensively studied. For instance, MIC by sulfate-reducing bacteria (SRB) was explained by the cathodic depolarization theory in early days [5–7]. Microbes can also produce corrosive metabolite such as organic acids and corrosive gases [8,9], or change oxygen concentration and pH at the solution/metal interface to enhance local corrosion [10–12]. Another key mechanism that has been more recently proposed to explain MIC is extracellular electron transfer (EET), which refers to the electron exchange process between microorganisms and extracellular electrodes such as metals [13–16].

Currently, EET studies are focused on dissimilatory metal-reducing bacteria (DMRB) such as the genus of *Shewanella*, *Bacillus* and *Pseudomonas* [17–19]. Generally, EET can be categorized as direct electron transfer (DET) or mediated electron transfer (MET). DET between bacterial cells and metals occurs via specific transmembrane proteins or

conductive nanowires [20–22]. For example, starved SRB was observed to heavily encrust and firmly attach to the carbon steel surface via nanowires to acquire electrons as the energy source to support their metabolism [23]. In MET, microbes exchange electrons with external electrodes through redox-active mediators as electron shuttles. MET allows microbes to transfer electrons without contact with the electrodes, which may expand the distance of electron transport [24]. Microorganisms can make use of electron shuttles present in environments repeatedly to facilitate EET. Electron shuttles can also be endogenously produced by bacteria such as flavins by *Shewanella* and phenazines by *Pseudomonas* [25–27].

Recent studies have shown that MIC can be accelerated by decreasing the availability of organic carbon source or electron acceptors depending on the state of the materials surface or by the addition of exogenous electron shuttles [28,29]. For example, Dou et al. demonstrated that *Desulfovibrio vulgaris* under organic carbon starvation caused more severe corrosion of C1018 carbon steel which served as an alternative energy source for bacterial growth [30]. Li et al. showed that the EET of *Bacillus licheniformis* on the X80 steel was enhanced under organic carbon starvation. [31]. In this study, 5-cyano-2,3-ditolyl

---

tetrazolium chloride (CTC) was used as an indicator of microbial respiration. The counterstaining of CTC-treated samples with 4′,6-diamidino-2-phenylindole (DAPI) was applied to directly reveal the reduction of CTC in cells by the electrons from extracellular X80 steel electrodes under nutrient-deprived conditions. Philips et al. demonstrated that *Shewanella* strain 4t3-1-2LB isolated from an acetogenic community enriched with Fe(0) as the sole electron donor completely reduced fumarate and caused a 7-fold increase in the corrosion rate in comparison with the abiotic control [32]. In a recent study, we showed that *S. oneidensis* MR-1 could accelerate the corrosion of 304 stainless steel via bidirectional EET mediated by exogenous RF. On the steel with intact passive surface, outward EET from *S. oneidensis* MR-1 could reduce Fe(III) oxides and caused passivity breakdown. On an abraded surface, the bacteria could accelerate the oxidation of the metallic Fe via an inward EET process [33].

The effects of microbes on corrosion are two-fold [34]. Besides the corrosion-accelerating effect of bacteria, microbes can directly or indirectly mitigate corrosion via processes known as microbiologically influenced corrosion inhibition (MICI) [35,36]. MICI can be achieved by microbial respiration consumption of corrosive substances, formation of mineralized layers, formation of EPS protective layer, competitive microbial corrosion inhibition or microbial secretion of corrosion inhibitors [37]. For example, Liu et al. showed that the EPS secreted by *Pseudoalteromonas lipolytica* strain could complex calcium ions in the environment and induced the deposition of a calcium carbonate mineralized layer to protect the steel surface from corrosion [38]. More recently, we showed that *Shewannella putrefaciens* could also inhibit corrosion of carbon steels via microbial mineralization of calcium carbonate [35]. *S. putrefaciens* cells preferred to colonize on steels and formed thicker biofilms under starvation of organic nutrients [39], although further study is needed to confirm whether EET could influence the MICI process.

This study aims to investigate the MIC of pure iron by *S. oneidensis* MR-1 in the presence of different levels of RF as mediators for the EET process. The corrosion behavior was studied by electrochemical impedance spectroscopy (EIS), linear polarization resistance (LPR), potentiodynamic polarization (PDP) curves and electrochemical noise (EN). Scanning electron microscopy (SEM) was employed to observe the surface morphology of pure iron after immersion with and without the bacteria. The compositions of the surface products were investigated by energy dispersive X-ray spectrometry (EDS) and X-ray diffraction (XRD). The concentrations of the dissolved Fe ions after corrosion were measured by inductively coupled plasma mass spectrometry (ICP-MS).

2. Experimental

2.1. Materials

Pure iron foil (99.5%) FE000470 was purchased from Goodfellow Cambridge Limited. Square coupons (10 mm × 10 mm × 3 mm), sealed with epoxy resin to expose only one surface (1 cm^2), were prepared for all experiments. The exposed surfaces were sequentially abraded by 240, 400, 600, 800 grit abrasive paper and cleaned with anhydrous ethanol under ultrasonication. Before tests, all coupons were sterilized under UV irradiation for 30 min.

2.2. Bacterium and culture medium

S. oneidensis MR-1 strain MCCC 1A01706 was obtained from the Marine Culture Collection of China (MCCC). All tests were carried out in *Shewanella* basal medium (SBM) with the following ingredients: 5.6 g/L sodium lactate, 3.2 g/L disodium fumarate, 4.78 g/L HEPES, 0.5 g/L casamino acid, 0.46 g/L NH_4Cl, 0.225 g/L K_2HPO_4, 0.225 g/L KH_2PO_4, 0.117 g/L $MgSO_4 \cdot 7H_2O$, 0.225 g/L $(NH_4)_2SO_4$ and 10 mL/L trace element solution. The composition of the trace element solution in 1000 mL deionized water was as follows: 1.5 g NTA, 0.1 g $MnCl_2 \cdot 4H_2O$, 0.3 g

$FeSO_4 \cdot 7H_2O$, 0.17 g $CoCl_2 \cdot 6H_2O$, 0.1 g $ZnCl_2$, 0.04 g $CuSO_4 \cdot 5H_2O$, 0.005 g $AlK(SO_4)_2 \cdot 12H_2O$, 0.005 g H_3BO_3, 0.09 g Na_2MoO_4, 0.12 g $NiCl_2$, 0.02 g $NaWO_4 \cdot 2H_2O$ and 0.10 g Na_2SeO_4. Prior to the autoclaving treatment (MLS-3781-PC, Panasonic) at 121 °C for 20 min, the pH of the medium was adjusted to 7.10 ± 0.03 by NaOH solution. Before immersion, 1 mL *S. oneidensis* MR-1 planktonic seed culture in LB medium (containing 10 g/L tryptone, 5 g/L yeast extract and 10 g/L NaCl) was inoculated into a flask containing 100 mL SBM. The bacteria were pre-grown at 30 °C for 10 h. Later, 0, 10 or 20 ppm RF was added to the medium and left for 15 min statically while the bacteria consumed oxygen. The deoxidization of the sterile medium was achieved by injecting pure nitrogen into SBM for 30 min. Three identical coupons were placed at the bottom of each flask in the anaerobic chamber (1029, Thermo Fisher Scientific) and then the flask was sealed with a rubber stopper. The optical density value at 600 nm (OD_{600}), which can be used to evaluate the growth of the planktonic cells, was measured by a UV spectrophotometer (Bio Mate3S, Thermo Fisher Scientific) [40].

2.3. Surface analysis

After immersion, the morphology of the biofilms on the coupon surfaces was observed by SEM (JSM-F100, JEOL). To fix the bacteria, the coupons were immersed in 2.5% (v/v) glutaraldehyde solution at 4 °C for 8 h after rinsing with phosphate buffer saline (PBS). The coupons were then sequentially dehydrated with ethanol solutions for 8 min under each concentration (50, 60, 70, 80, 90, 100, 100, 100 vol%). The coupons were further dried in air and sputter-coated with Au to improve the conductivity of surfaces before SEM observation. The composition of the surface products after immersion was investigated by grazing incidence X-ray diffraction (XRD, Empyrean, Malvern Panalytical). After 7 days of immersion in the inoculated media, the biofilm on the coupons was removed with sterile cotton swabs immediately. The coupons were then rinsed with sterile deionized water in the anaerobic chamber, and finally stored in an air-tight vacuum desiccator. Control coupons were also rinsed with sterile deionized water and stored as mentioned above. The incidence angle of the XRD measurements was set to 1.5° to avoid an exorbitant Fe peak occurrence. Peak shape analysis and phase identification were carried out using MDI Jade software (Version 6.2).

2.4. ICP-MS analysis

The concentration of the dissolved Fe ions from the coupons was evaluated by inductively coupled plasma mass spectrometry (ICP-MS, ICPOES730, Agilent). The biotic and abiotic SBM were pretreated with concentrated nitric acid (65 wt%) at 80 °C for 30 min. ICP-MS was operated at a plasma flow rate of 15 L/min, an auxiliary gas flow rate of 1.5 L/min and a nebulizer gas flow rate of 0.75 L/min. The radio frequency power was 1000 W and the helium was utilized as the carrier gas.

2.5. Electrochemical tests

The electrochemical tests were conducted under anaerobic conditions similar to the immersion tests as mentioned in section 2.2. The electrochemical station (Reference 600 Plus, Gamry) controlled by ESA410 software in a zero resistance ammeter (ZRA) mode was used to perform the electrochemical noise tests. Two basically identical iron coupons were used as the working electrode and the counter electrode. A saturated calomel electrode (SCE) was used as the reference electrode [41]. The sampling frequency was 20 Hz and the sampling time was set to 15 min after immersion for 0 h, 4 h, 8 h, and 12 h.

Gamry Reference 600 Plus controlled by framework software was used to conduct other electrochemical tests with a conventional three-electrode system consisting of an iron coupon as the working electrode, a platinum foil as the counter electrode and an SCE as the reference electrode. Open circuit potential (OCP) was first measured for 1 h
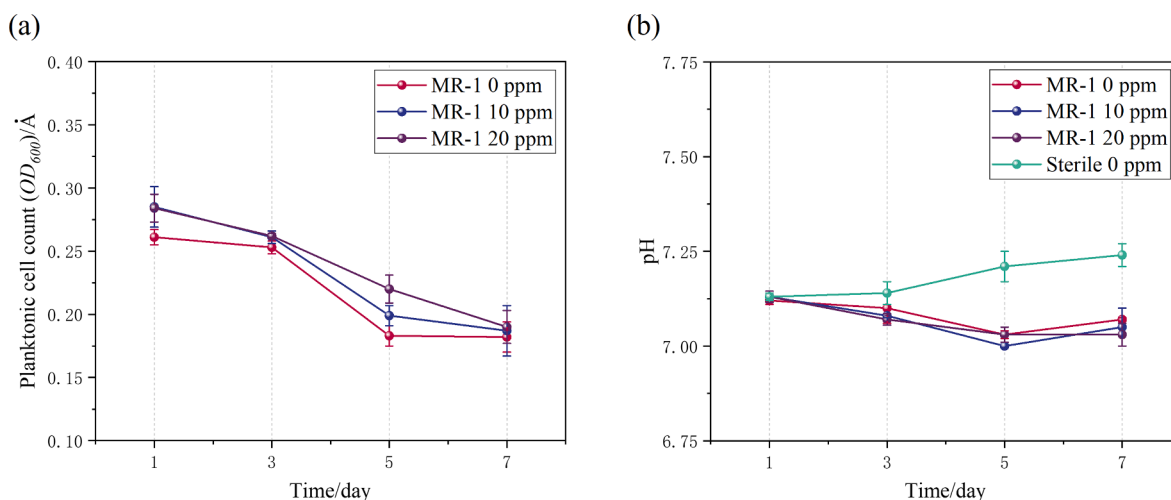
Fig. 1. (a) Growth curves of planktonic MR-1 in the SBM with various RF concentrations; (b) pH variation of the SBM containing MR-1 strains with various RF concentrations and the sterile control.
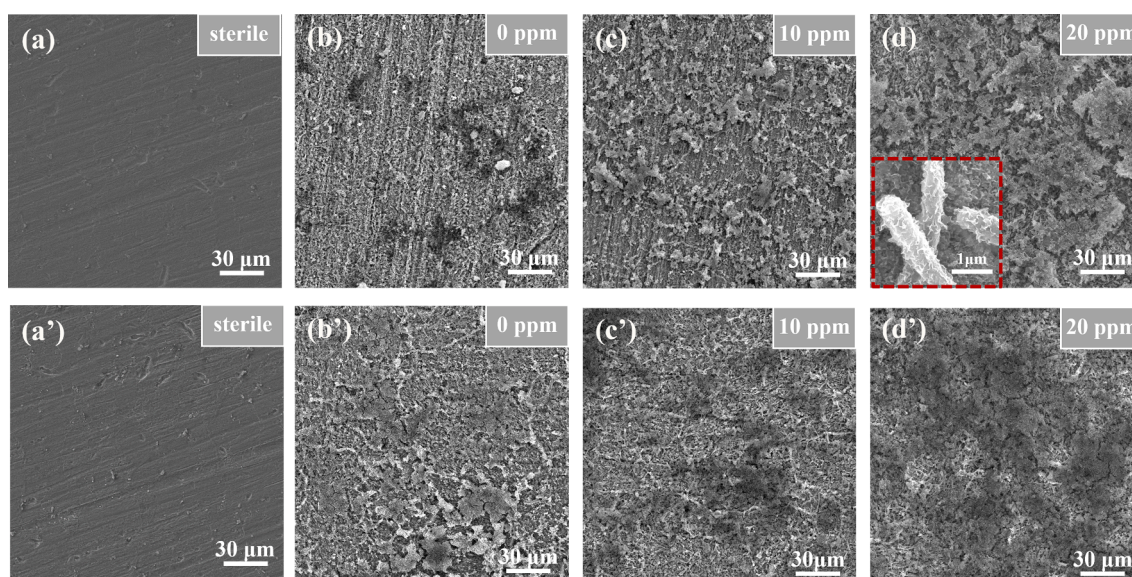

Fig. 2. (a-d) SEM images of the surface products on the coupons in the sterile medium and the inoculated media with RF concentrations of 0 ppm, 10 ppm and 20 ppm after 3 days and (a'-d') 7 days.

to ensure that the system had reached a steady status. LPR was carried out at a scanning rate of 0.125 mV/s from -10 mV to 10 mV vs. E_{OCP}. EIS was taken with 10 mV amplitude sinusoidal perturbation vs. E_{OCP} in the frequency range of 10^5-10^{-2} Hz. EIS results were analyzed by ZSimpWin software (Version 3.50). PDP curves were measured from -200 mV to 200 mV vs. E_{OCP} with a scanning rate of 2 mV/s after 7 days of immersion. The PDP results were analyzed with EC-Lab software (Version 9.32).

3. Results and discussion

3.1. Bacterial growth

Fig. 1a shows the growth curves of the planktonic bacteria during the 7 days of immersion in the culture media with various RF concentrations. The growth curves show minimal difference with 10 ppm or 20 ppm RF added to the medium, which suggests that RF does not affect the growth of the planktonic bacteria. Fig. 1b shows the pH variation of the bacteria-inoculated media with different RF concentrations and the

sterile control. The pH values of the inoculated media were ~ 7 after 7 days, which was slightly lower than that of the sterile control (pH = 7.25). The addition of RF did not affect the pH values of the inoculated media. Based on the previous work [33], RF had no corrosion promoting or inhibiting effect on the steel surface in the sterile condition. Therefore, the corrosion behaviors of pure iron in the sterile medium with various RF concentrations were not considered in this study.

3.2. Corrosion morphology

Fig. 2 shows the morphology of the surface products on the pure iron coupons after immersion in the sterile and inoculated media with various RF concentrations for 3 and 7 days. In Fig. 2a and a', the iron surface was free of corrosion products after immersion in the sterile medium. In contrast, a significant amount of corrosion products was observed on the surfaces of coupons immersed in the inoculated media and became higher with an increased RF concentration (Fig. 2b-d). The corrosion products continued to accumulate after 7 days of immersion (Fig. 2b'-d'). In the presence of 20 ppm RF, the corrosion product
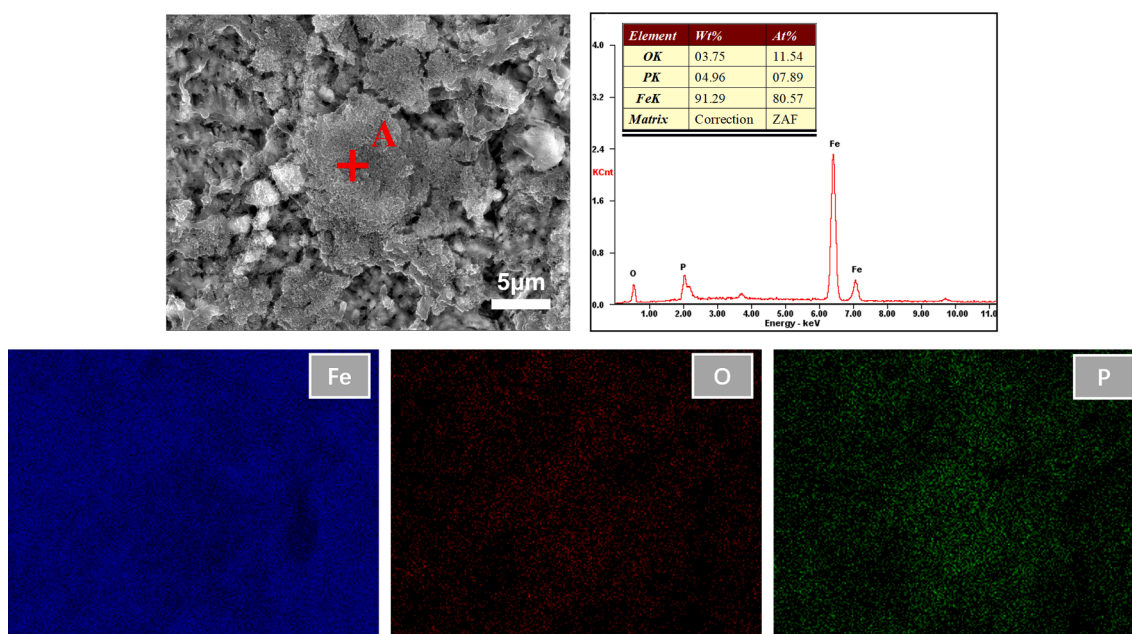
Fig. 3. SEM image and EDS spectrum of corrosion products on the pure iron coupon after 7 days of immersion.
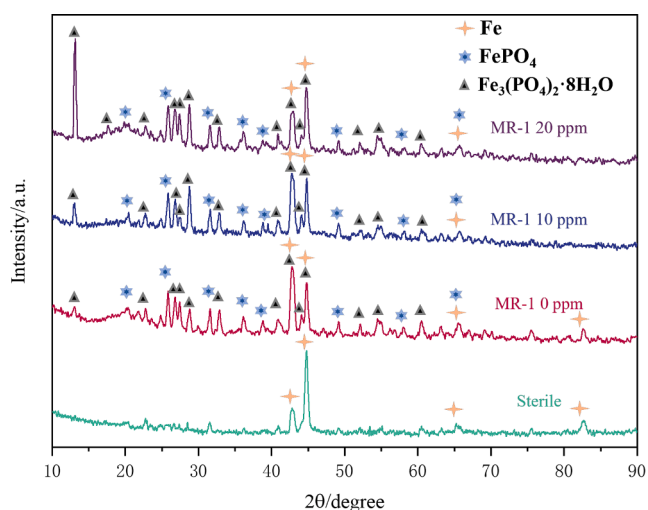

Fig. 4. XRD pattern of the pure iron coupons after 7 days of immersion in the sterile medium and the inoculated media with various RF concentrations.
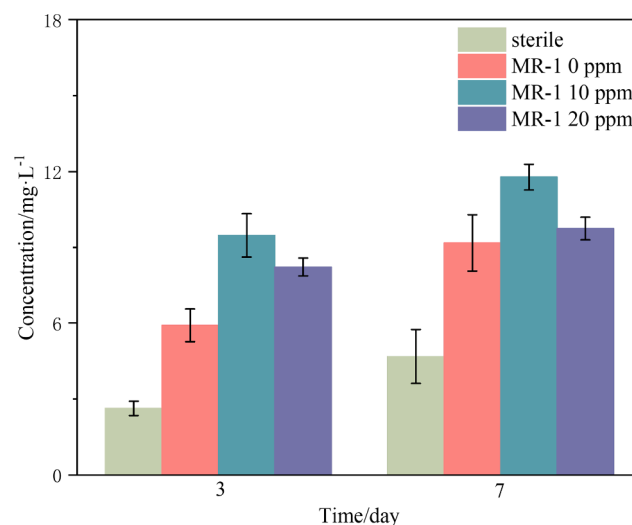

Fig. 5. The concentration of dissolved Fe in the sterile medium and MR-1 inoculated media with various RF concentrations after immersion for 3 days and 7 days.

formed a uniform layer that completely covered the iron surface (Fig. 2**d'**). After 3 days of immersion (Fig. 2**d**), the enlarged SEM image revealed that lamellar corrosion products were also attached to the cell wall, which implied that the surface of bacteria could also serve as nucleation sites of the corrosion product.

3.3. Composition of corrosion products

Fig. 3 shows the SEM images and EDS results of the corrosion products on the iron surface after 7 days of immersion in the inoculated medium (0 ppm RF). The EDS analysis shows a high level of P, O and Fe elements on the corrosion products. The EDS mapping reveals an intense and uniform Fe signal, and the enrichment of O and particularly P elements at the sites of corrosion products. According to the results from the grazing incidence XRD (Fig. 4), the corrosion products on the coupon surface in the presence of the bacteria were mainly composed of $Fe_3(PO_4)_2 \cdot 8H_2O$ and a minor level of $FePO_4$. The intensity of the peak at the 2θ value of ~13.1°, corresponding to the lattice indices (0 2 0) of

$Fe_3(PO_4)_2 \cdot 8H_2O$, increased significantly with the RF concentration. The formation of a minor level of $FePO_4$ may have resulted from the exposure of Fe (II) phosphate to oxygen prior to the XRD test. In contrast, only the characteristic peak of iron was observed in the XRD results of the surface after immersion in the sterile medium. These results combined with the SEM images indicated that the corrosion of pure iron was significantly promoted in the presence of *S. oneidensis* MR-1. Moreover, the addition of exogenous RF as electron transfer mediators enhanced this process and formed more corrosion products mainly composed of $Fe_3(PO_4)_2 \cdot 8H_2O$.

3.4. ICP-MS results

Fig. 5 presents the Fe ions leaching results of the coupons immersed in the sterile and the inoculated media for 3 days and 7 days. After 3 days of immersion in the inoculated medium with 0 ppm exogenous RF, the
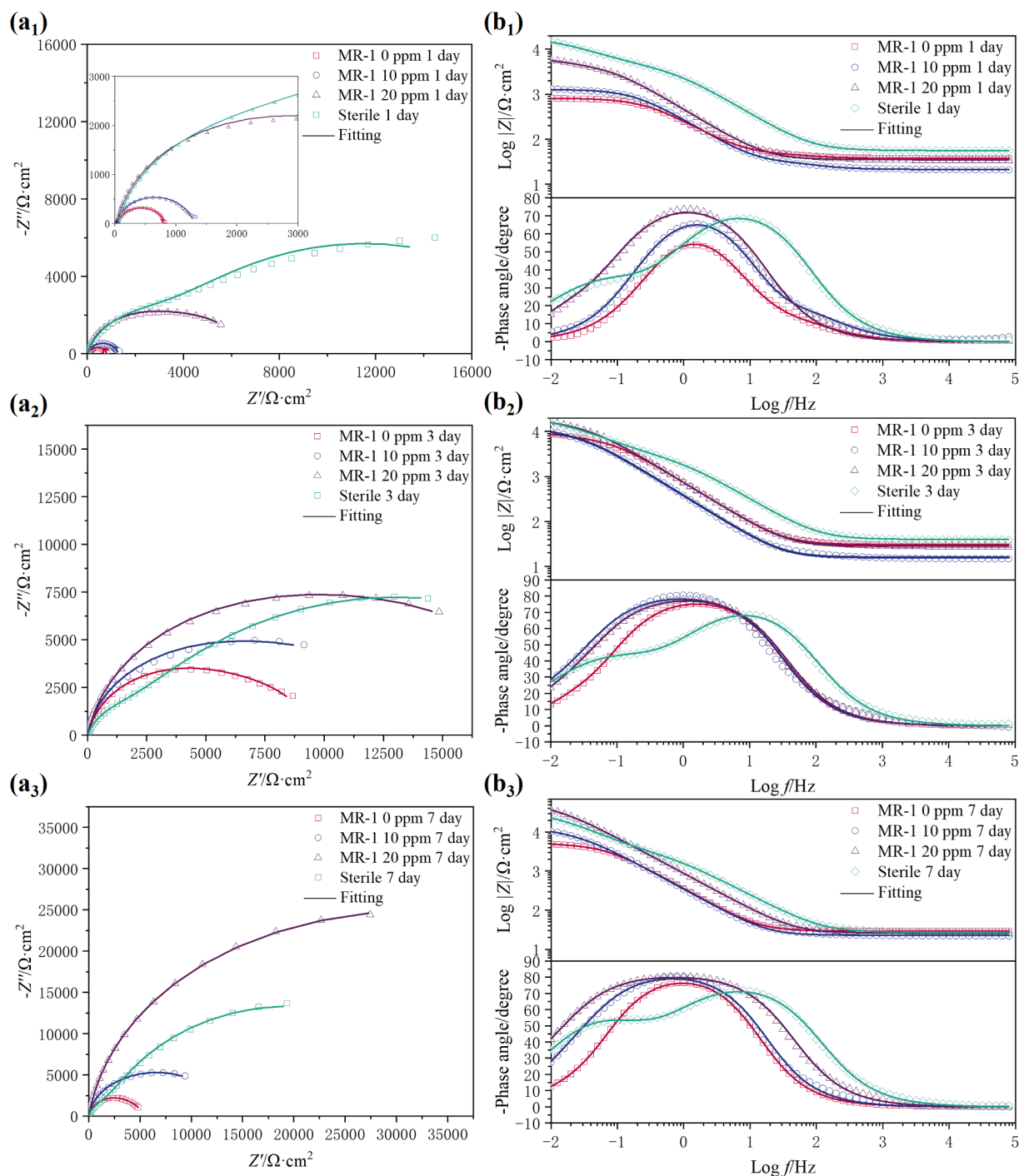
Fig. 6. Nyquist and Bode plots for the coupons immersed in the sterile medium and the MR-1 inoculated media with various RF concentrations for 1 (a_1, b_1), 3 (a_2, b_2) and 7 (a_3, b_3) days.

amount of Fe ions reached 5.91 mg/L, which was over twice of that in the sterile medium (2.63 mg/L). With the addition of 10 ppm and 20 ppm RF under biotic conditions, the corresponding Fe ion concentrations were 9.48 mg/L and 8.22 mg/L, respectively. The addition of exogenous RF induced faster Fe dissolution. The lower level of dissolved Fe ions with 20 ppm RF may be attributed to the deposition of dissolved Fe and the formation of protective corrosion product layer. After 7 days, the concentration of Fe ions reached 4.68 mg/L in the sterile medium and 9.18 mg/L in the inoculated medium without RF. The concentrations of Fe ions in the media with 10 ppm RF (11.78 mg/L) and 20 ppm RF (9.75 mg/L) were still higher than that in the medium without RF,

but their increments were smaller than that for the 0 ppm RF group. The ICP-MS results confirmed that MIC was enhanced with the addition of exogenous RF. The increased amount of RF induced the formation of a continuous corrosion product layer that may suppress the corrosion.

3.5. Electrochemical tests

Fig. 6 shows the EIS results of pure iron in the sterile medium and the inoculated media with 0 ppm, 10 ppm, and 20 ppm RF. After 1 day, the diameter of the semicircles in the Nyquist plots for the coupons in the inoculated media were smaller than that in the sterile medium,
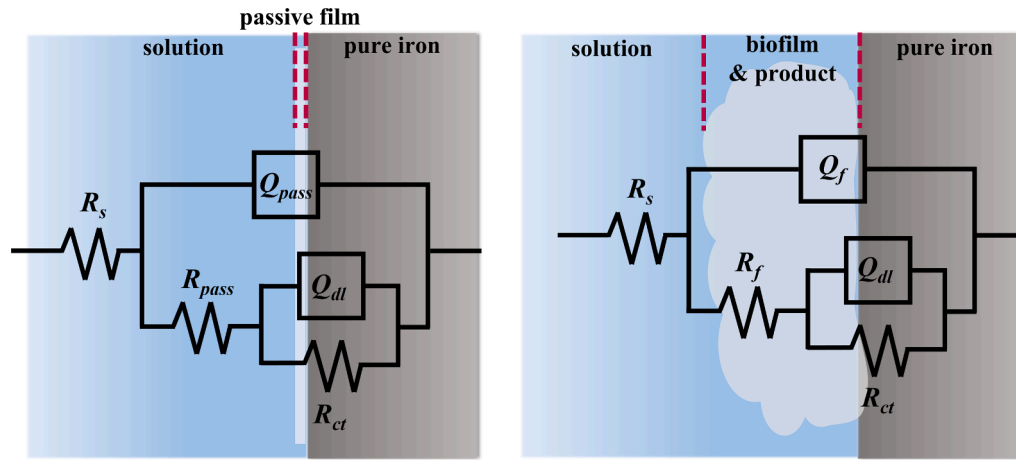
Fig. 7. The electrical equivalent circuits used to fit the EIS spectra.

Table 1
EIS parameters for coupons in the inoculated media.

Type	Time	R_s	$Q_f \times 10^{-4}$	R_f	$Q_{dl} \times 10^{-4}$	R_{ct}	$\chi^2 \times 10^{-4}$
—	(day)	(Ω cm²)	(Ω^{-1} cm^{-2} S^n)	(kΩ cm²)	(Ω^{-1} cm^{-2} S^n)	(kΩ cm²)	—
MR-1 0 ppm	1	38.2 ± 0.7	1.8 ± 1.4	0.03 ± 0.01	4.7 ± 0.2	0.8 ± 0.01	5.8 ± 2.7
	3	30.5 ± 0.2	2.8 ± 0.3	6.6 ± 1.2	149 ± 100	1.3 ± 0.3	1.6 ± 0.2
	7	29.8 ± 0.5	4.7 ± 0.2	5.0 ± 0.2	149 ± 40.4	0.7 ± 0.2	1.5 ± 0.6
MR-1 10 ppm	1	22.9 ± 1.7	3.1 ± 0.8	0.02 ± 0.01	4.1 ± 0.9	1.3 ± 0.03	43.9 ± 38.7
	3	18.1 ± 2.3	4.8 ± 0.05	11.5 ± 1.3	45.0 ± 1.6	3.4 ± 0.4	47.9 ± 4.2
	7	23.4 ± 0.5	5.1 ± 0.07	10.6 ± 0.2	29.9 ± 1.9	2.8 ± 0.2	25.8 ± 1.2
MR-1 20 ppm	1	34.3 ± 0.7	4.2 ± 0.06	5.0 ± 0.1	51.6 ± 3.6	1.7 ± 0.01	35.0 ± 4.6
	3	31.1 ± 2.8	3.0 ± 0.4	13.5 ± 2.1	31.9 ± 7.8	4.0 ± 0.2	19.8 ± 5.4
	7	26.1 ± 0.1	2.1 ± 0.02	61.0 ± 9.1	14.9 ± 7.1	17.1 ± 6.6	9.5 ± 0.9

Table 2
EIS parameters for coupons in the sterile medium.

Type	Time	R_s	$Q_{pass} \times 10^{-4}$	R_{pass}	$Q_{dl} \times 10^{-4}$	R_{ct}	$\chi^2 \times 10^{-4}$
—	(day)	(Ω cm²)	(Ω^{-1} cm^{-2} S^n)	(kΩ cm²)	(Ω^{-1} cm^{-2} S^n)	(kΩ cm²)	—
Sterile	1	47.0 ± 8.9	0.6 ± 0.06	2.6 ± 0.05	1.8 ± 0.2	18.9 ± 0.2	4.0 ± 1.2
	3	33.7 ± 6.1	0.8 ± 0.02	3.5 ± 0.2	2.1 ± 0.4	19.8 ± 1.7	3.0 ± 0.5
	7	27.6 ± 0.5	0.9 ± 0.1	4.0 ± 0.06	1.8 ± 0.2	20.9 ± 2.5	3.3 ± 0.9

sterile medium, including one for the formation of a passive film and the other for the charge transfer process of iron corrosion [42]. The phase angle plots of the coupons in the inoculated media exhibited a broad peak in the medium to low frequency region, which could be associated with the formation of phosphate layer in the presence of bacteria and the charge transfer process on iron surface. It is noteworthy that the Nyquist and Bode plots of the coupons in the sterile medium changed little over time, which agreed with the SEM observation (Fig. 2a and a').

The electrical equivalent circuits shown in Fig. 7 were used to fit the EIS data, and the specific fitted parameters were summarized in Tables 1 and 2. In the circuits, R_s represents the solution resistance; Q_f is the constant phase element (CPE) used to simulate the capacitance of the surface film consisting of the biofilm and the corrosion products; Q_{dl} is capacitance of the electrical double layer. R_f and R_{ct} reflect the resistance of the surface film and the charge transfer resistance, respectively. For the sterile control, Q_{pass} was used as the capacitance of the passive film [42]. A CPE is usually used instead of a pure capacitance to fit non-ideal films on the surface. The impedance of CPE is defined by the following relation:

$$Z = \frac{1}{Q} (j\omega)^{-n} \tag{1}$$

where Q and n is the magnitude and the exponent constant of CPE, respectively; j is the imaginary number; ω is the angular frequency.

In Table 2, the R_{ct} values of the coupons immersed in the sterile medium were approximately 20 kΩ cm² during the entire 7 days. In the inoculated media, the R_{ct} values were significantly lower at the initial stage of immersion than that in the sterile medium, which confirmed that the corrosion-accelerating effect of *S. oneidensis* MR-1 on the pure iron. However, the values of R_{ct} and R_f increased obviously with the increase of immersion time and the addition of more RF. After 7 days, the R_f values of the coupons immersed in the media containing 0 ppm, 10 ppm and 20 ppm RF reached 5.0 kΩ cm², 10.6 kΩ cm² and 61.0 kΩ cm², respectively. The results revealed that the corrosion product layer formed in the inoculated media exhibited good protective properties. The addition of 20 ppm RF induced the formation of a dense protective layer and therefore showed the highest corrosion resistance.

LPR is a classical method for fast corrosion analysis and is mostly used for corrosion conditions that change frequently over a short period of time [43]. R_p values were calculated by dividing the applied overpotential (-10 mV to $+10$ mV vs. E_{OCP}) by the induced current. Fig. 8a shows the R_p values for the coupons immersed in the sterile medium and the inoculated media with various RF concentrations. The R_p value of the coupons immersed in the sterile medium stayed around 20 kΩ cm² during the 7 days of immersion, which was consistent with the EIS results. With 0 ppm and 10 ppm RF added in the inoculated media, the R_p

indicating that the presence of the bacteria accelerated the corrosion of pure iron during the early stage. Correspondingly, the impedance modulus at the low-frequency region ($|Z|_{0.01Hz}$) in the Bode plots, which is commonly used as a semi-quantitative indicator of corrosion resistance [39], was lower for the coupons in the inoculated media. With the increase of immersion time, the diameters of semicircles and the $|Z|_{0.01Hz}$ values increased gradually for the coupons in the inoculated media, especially in the medium containing 20 ppm RF. Two time constants were observed in the phase angle plots of the coupons in the
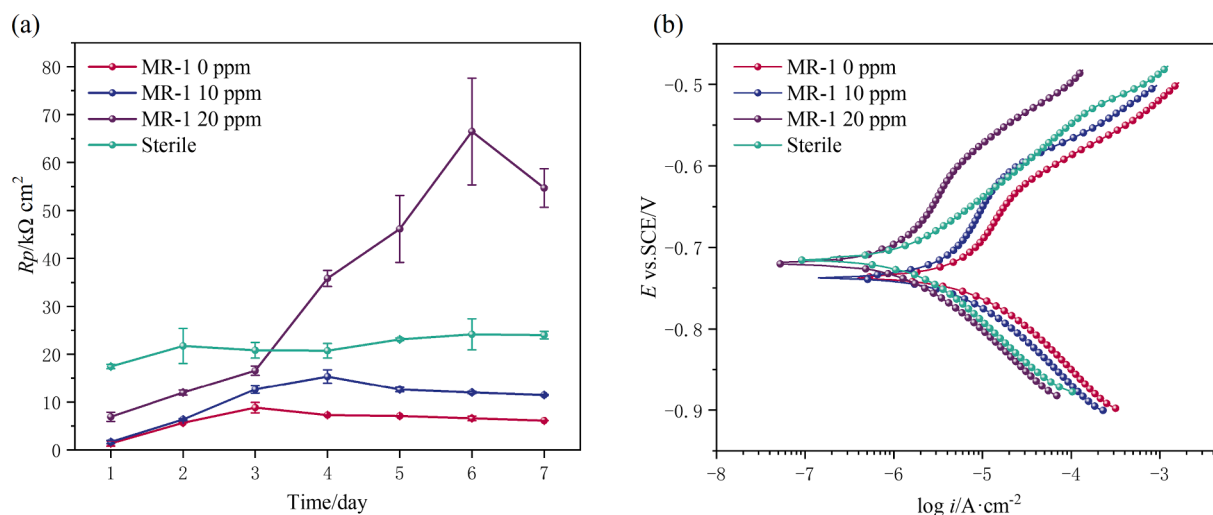
(a)

(b)

Fig. 8. (a) LPR results and (b) PDP curves of pure iron immersed in sterile medium and inoculated media containing MR-1 with various RF concentrations.

Table 3
Electrochemical corrosion parameters determined from the PDP curves.

	E_{corr} (V vs. SCE)	i_{corr} (μA cm^{-2})
MR-1 0 ppm	-0.74 ± 0.02	5.5 ± 0.1
MR-1 10 ppm	-0.74 ± 0.01	3.7 ± 0.1
MR-1 20 ppm	-0.72 ± 0.02	0.9 ± 0.2
Sterile	-0.71 ± 0.02	1.5 ± 0.1

values slightly increased in the beginning and then stabilized but were always lower than those for the sterile control. The highest R_p value was observed in the medium containing 20 ppm RF, which increased from 6.9 kΩ cm^2 after 1 day to 54.7 kΩ cm^2 after 7 days.

Fig. 8**b** shows the PDP curves of the coupons immersed in the sterile medium and the inoculated media after 7 days of immersion. The corresponding electrochemical parameters, including the corrosion potential (E_{corr}) and the corrosion current density (i_{corr}), obtained from the PDP curves by the extrapolation of the Tafel slope in cathodic branch, are summarized in Table 3. When the RF concentration increased from 0 ppm to 20 ppm, the anodic branch of the curve moved to the negative direction in the presence of MR-1, suggesting that the anodic reactions were suppressed. The i_{corr} value also decreased with the addition of more RF, which was consistent with the EIS and LPR results. In the presence of bacteria, a pseudo-passivation region was observed in the anodic branch of the polarization curve, which was associated with the formation of the corrosion product layer [44].

The results above suggested that the corrosion of pure iron was promoted in the early stage (1 to 3 days) because of the presence of the bacteria. With extended immersion, the corrosion process was suppressed as the bacteria gradually formed an iron phosphate layer with good protective properties on the coupon surface. Even after only 1 day, the better protective properties could be observed when a higher amount of RF was added. In the entire immersion process, the coupons immersed in the inoculated medium containing 20 ppm RF always exhibited higher corrosion inhibition properties than those in the media containing 0 ppm and 10 ppm RF.

EN testing was used to further study the corrosion of iron surface at the initial stage of immersion (0 to 12 h). As a fully passive monitoring technique, EN measurement has less impact on cell growth and biofilm thickness than continuous EIS and LPR measurements, and is a particularly suitable method to continuously monitor MIC [45–47]. The standard statistical parameters, containing the standard deviations current (σ_I) and potential (σ_V) fluctuations, can be utilized to describe the amplitude of current and potential noise signal in the time domain
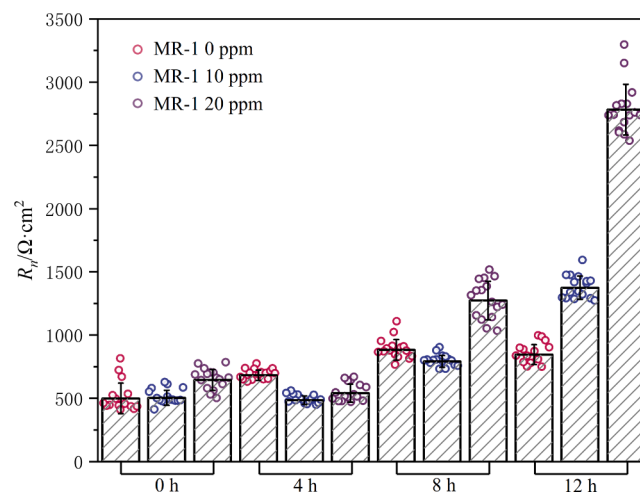

Fig. 9. The noise resistance of coupons immersed in the inoculated media with 0 ppm, 10 ppm and 20 ppm RF.

[48]. The noise resistance (R_n) is defined as the ratio between σ_V and σ_I, which has a good correlation with the R_p value obtained from LPR. A higher R_n value indicates a lower corrosion rate [49]. The EN test of each electrochemical cell was monitored for 15 min, in which a set of R_n values were obtained every 50 s after waiting for 100 s for the system to stabilize. Fig. 9 shows the R_n values of the coupons immersed in the inoculated media with various RF concentrations. The R_n values at 0 h were low and unstable. At this time, the coupons were just immersed in the media and the bacteria cells began to attach to the surface. The data after 4 h of immersion showed that the R_n values of the coupons with 10 ppm and 20 ppm RF were $\sim$ 500 Ω cm^2, which were lower than that of the sterile control. By this time, the bacteria have colonized the surface of the coupons and performed EET using exogenous RF, resulting in the reduction in the R_n values. After 8 h, the R_n values of the coupon immersed in the medium with 20 ppm RF was higher than those of the others. After 12 h, the R_n values of the coupons with 0 ppm, 10 ppm and 20 ppm RF were 842.7 Ω cm^2, 1372.1 Ω cm^2 and 2788.9 Ω cm^2, respectively. The EN results suggested that the increase of the RF concentration promoted the rate of MIC at the initial stage of immersion. However, the accelerated corrosion also induced more significant deposition of the corrosion products.
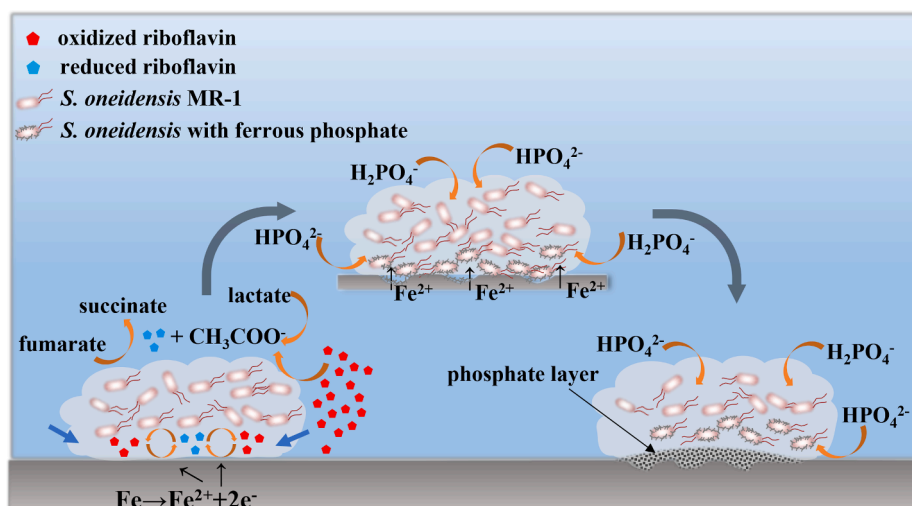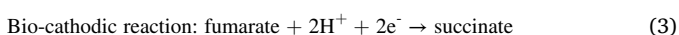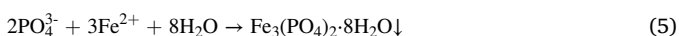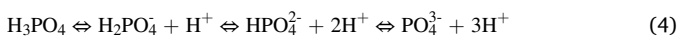
Fig. 10. Schematic diagram of phosphate deposition by *S. oneidensis* MR-1.

3.6. MIC mechanism

The study showed that the presence of *S. oneidensis* MR-1 could accelerate the corrosion pure iron in an anaerobic environment. However, the addition of exogenous RF, which is a redox-active mediator facilitating the EET process between *S. oneidensis* MR-1 and iron surface, induces a MICI effect by generating a protective phosphate layer on the iron surface. Fig. 10 presents the schematic diagram of phosphate deposition after corrosion induced by *S. oneidensis* MR-1. In the bacterial medium, sodium lactate was used as carbon source to participate in respiratory metabolism of MR-1. Fumarate was the final electron acceptor since oxygen is absent in the culture environment. The following redox reactions took place in the MIC process on the iron surface when the carbon source is consumed or insufficient as the biofilm may prevent the diffusion of organic carbon nutrients [33]:

Anodic reaction: $Fe \rightarrow Fe^{2+} + 2e^-$ (2)

Bio-cathodic reaction: $fumarate + 2H^+ + 2e^- \rightarrow succinate$ (3)

According to the previous work, the electrons produced by iron oxidation were carried by reduced RF and then transferred through bacterial surface membrane proteins to the cell interior for consumption by the reaction with fumarate. This process would provide energy for the bacteria and the oxidized RF would continue to participate in EET. The ICP-MS results confirmed that the increase of exogenous RF in the solution could accelerate MIC of iron by enhancing the EET process (Fig. 5). The EN results further indicated that the R_n values of the coupons immersed in the inoculated media with RF were lower than for those without RF at the initial stage (Fig. 9), indicating a higher corrosion rate. The dissolved Fe(II) ions react with the phosphate ions in the culture medium and rapidly induce the deposition of a layer of ferrous phosphate on the iron surface [50]:

$$H_3PO_4 \Leftrightarrow H_2PO_4^- + H^+ \Leftrightarrow HPO_4^{2-} + 2H^+ \Leftrightarrow PO_4^{3-} + 3H^+$$ (4)

$$2PO_4^{3-} + 3Fe^{2+} + 8H_2O \rightarrow Fe_3(PO_4)_2 \cdot 8H_2O\downarrow$$ (5)

The results from the electrochemical tests and ICP-MS supported that, with the increase of RF, microbes accelerated the dissolution of Fe to Fe(II) ions which was a driving force of ferrous phosphate deposition. This phosphate layer could not form on the coupon surface in the sterile medium due to the extremely low corrosion rate (Fig. 2).

4. Conclusions

This work investigated the influence of RF as an EET mediator on corrosion of pure iron induced by *S. oneidensis* MR-1. The presence of RF did not affect the cell growth as well as the pH of media. The results from SEM and XRD image confirmed that a ferrous phosphate layer was generated on the iron surface. The coverage and amount of the ferrous phosphate layer increased with higher additions of RF. The ICP-MS results revealed that corrosion of the iron coupons was accelerated in the inoculated media at the initial stage in the presence of 10 and 20 ppm RF, which was consistent with EN results. The EIS, LPR and PDP results showed that the phosphate layer exhibited good protection performance and gradually inhibited the corrosion of coupons with immersion time, especially in the presence of 20 ppm RF. The addition of RF promotes the microbiologically induced phosphate deposition by *S. oneidensis* MR-1 on iron surface, which may be valuable for the development of a greener alternative approach to conventional phosphate conversion coatings.

Declaration of Competing Interest

The authors declare that they have no known competing financial interests or personal relationships that could have appeared to influence the work reported in this paper.

Acknowledgement

References

[1] B.J. Little, J.S. Lee, Microbiologically influenced corrosion: an update, Int. Mater. Rev. 59 (7) (2014) 384–393.

[2] N. Kip, J.A. van Veen, The dual role of microbes in corrosion, Isme J. 9 (3) (2015) 542–551.

[3] S.Q. Chen, P. Wang, D. Zhang, Corrosion behavior of copper under biofilm of sulfate-reducing bacteria, Corros. Sci. 87 (2014) 407–415.

[4] E.Z. Zhou, J.J. Wang, M. Moradi, H.B. Li, D.K. Xu, Y.T. Lou, J.H. Luo, L.F. Li, Y. L. Wang, Z.G. Yang, F.H. Wang, J.A. Smith, Methanogenic archaea and sulfate reducing bacteria induce severe corrosion of steel pipelines after hydrostatic testing, J. Mater. Sci. Technol. 48 (2020) 72–83.

[5] M. Mehanna, I. Rouvre, M.L. Delia, D. Feron, A. Bergel, R. Basseguy, Discerning different and opposite effects of hydrogenase on the corrosion of mild steel in the presence of phosphate species, Bioelectrochemistry 111 (2016) 31–40.

[6] B.J. Little, J. Hinks, D.J. Blackwood, Microbially influenced corrosion: towards an interdisciplinary perspective on mechanisms, Int. Biodeter. Biodegr. 154 (2020).

[7] J. Li, C. Du, Z. Liu, X. Li, Electrochemical studies of microbiologically influenced corrosion of X80 steel by nitrate-reducing Bacillus licheniformis under anaerobic conditions, J. Mater. Sci. Technol. 118 (2022) 208–217.

[8] D. Liu, H.Y. Yang, J.H. Li, J.Q. Li, Y.Z. Dong, C.T. Yang, Y.T. Jin, L. Yassir, Z. Li, D. Hernandez, D.K. Xu, F.H. Wang, E.S.C.A. Smith, Electron transfer mediator PCN secreted by aerobic marine Pseudomonas aeruginosa accelerates microbiologically influenced corrosion of TC4 titanium alloy, J. Mater. Sci. Technol. 79 (2021) 101–108.

[9] Y. Liang, C. Li, P. Wang, D. Zhang, Fabrication of a robust slippery liquid infused porous surface on Q235 carbon steel for inhibiting microbiologically influenced corrosion, Colloid Surface A 631 (2021) 127696.

[10] Y. Lou, C. Dai, W. Chang, H. Qian, L. Huang, C. Du, D. Zhang, Microbiologically influenced corrosion of FeCoCrNiMo0.1 high-entropy alloys by marine Pseudomonas aeruginosa, Corros. Sci. 165 (2020) 108390.

[11] E. Gardin, S. Zanna, A. Seyeux, D. Mercier, A. Allion-Maurer, P. Marcus, Early stage of marine biofilm formation on duplex stainless steel, Biointerphases 15 (4) (2020) 041014.

[12] S. Pourhashem, A. Seif, F. Saba, E.G. Nezhad, X. Ji, Z. Zhou, X. Zhai, M. Mirzaee, J. Duan, A. Rashidi, B. Hou, Antifouling nanocomposite polymer coatings for marine applications: a review on experiments, mechanisms, and theoretical studies, J. Mater. Sci. Technol. 118 (2022) 73–113.

[13] G.P. Krantz, K. Lucas, E.L. Wunderlich, L.T. Hoang, R. Avci, G. Siuzdak, M. W. Fields, Bulk phase resource ratio alters carbon steel corrosion rates and endogenously produced extracellular electron transfer mediators in a sulfate-reducing biofilm, Biofouling 35 (2019) 669–683.

[14] H.-Y. Tang, D.E. Holmes, T. Ueki, P.A. Palacios, D.R. Lovley, E.T. Papoutsakis, Iron corrosion via direct metal-microbe electron transfer, Mbio 10 (3) (2019) e00303-19.

[15] L. Zhu, J. Wu, D. Zhang, P. Wang, Z. Sun, C. Li, E. Li, Influence of the α fraction on 2205 duplex stainless steel corrosion affected by Pseudomonas aeruginosa, Corros. Sci. 193 (2021) 109877.

[16] D.i. Wang, P. Kijkla, M.E. Mohamed, M.A. Saleh, S. Kumseranee, S. Punpruk, T. Gu, Aggressive corrosion of carbon steel by Desulfovibrio ferrophilus IS5 biofilm was further accelerated by riboflavin, Bioelectrochemistry 142 (2021) 107920.

[17] X.B. Liu, L. Shi, J.D. Gu, Microbial electrocatalysis: redox mediators responsible for extracellular electron transfer, Biotechnol. Adv. 36 (2018) 1815–1827.

[18] Z. Li, J. Wang, Y.Z. Dong, D.K. Xu, X.H. Zhang, J.H. Wu, T.Y. Gu, F.H. Wang, Synergistic effect of chloride ion and Shewanella algae accelerates the corrosion of Ti-6Al-4V alloy, J. Mater. Sci. Technol. 71 (2021) 177–185.

[19] I. Vassilev, N.J.H. Averesch, P. Ledezma, M. Kokko, Anodic electro-fermentation: empowering anaerobic production processes via anodic respiration, Biotechnol. Adv. 48 (2021) 107728.

[20] G. Reguera, K.D. McCarthy, T. Mehta, J.S. Nicoll, M.T. Tuominen, D.R. Lovley, Extracellular electron transfer via microbial nanowires, Nature 435 (2005) 1098–1101.

[21] Y.A. Gorby, S. Yanina, J.S. McLean, K.M. Rosso, D. Moyles, A. Dohnalkova, T. J. Beveridge, I.S. Chang, B.H. Kim, K.S. Kim, D.E. Culley, S.B. Reed, M.F. Romine, D.A. Saffarini, E.A. Hill, L. Shi, D.A. Elias, D.W. Kennedy, G. Pinchuk, K. Watanabe, S. Ishii, B. Logan, K.H. Nealson, J.K. Fredrickson, Electrically conductive bacterial nanowires produced by Shewanella oneidensis strain MR-1 and other microorganisms, Proc. Natl. Acad. Sci. U. S. A. 103 (30) (2006) 11358–11363.

[22] Y. Yang, Y. Ding, Y. Hu, B. Cao, S.A. Rice, S. Kjelleberg, H. Song, Enhancing bidirectional electron transfer of Shewanella oneidensis by a synthetic flavin pathway, Acs Synth. Biol. 4 (7) (2015) 815–823.

[23] B.W.A. Sherar, I.M. Power, P.G. Keech, S. Mitlin, G. Southam, D.W. Shoesmith, Characterizing the effect of carbon steel exposure in sulfide containing solutions to microbially induced corrosion, Corros. Sci. 53 (3) (2011) 955–960.

[24] E. Marsili, D.B. Baron, I.D. Shikhare, D. Coursolle, J.A. Gralnick, D.R. Bond, Shewanella Secretes flavins that mediate extracellular electron transfer, Proc. Natl. Acad. Sci. U. S. A. 105 (10) (2008) 3968–3973.

[25] H. von Canstein, J. Ogawa, S. Shimizu, J.R. Lloyd, Secretion of flavins by Shewanella species and their role in extracellular electron transfer, Appl. Environ. Microb. 74 (3) (2008) 615–623.

[26] L. Huang, Y. Huang, Y. Lou, H. Qian, D. Xu, L. Ma, C. Jiang, D. Zhang, Pyocyanin-modifying genes phzM and phzS regulated the extracellular electron transfer in microbiologically-influenced corrosion of X80 carbon steel by Pseudomonas aeruginosa, Corros. Sci. 164 (2020) 108355.

[27] L. Huang, W. Chang, D. Zhang, Y. Huang, Z. Li, Y. Lou, H. Qian, C. Jiang, X. Li, A. Mol, Acceleration of corrosion of 304 stainless steel by outward extracellular electron transfer of Pseudomonas aeruginosa biofilm, Corros. Sci. 199 (2022) 110159.

[28] P.Y. Zhang, D.K. Xu, Y.C. Li, K. Yang, T.Y. Gu, Electron mediators accelerate the microbiologically influenced corrosion of 304 stainless steel by the Desulfovibrio vulgaris biofilm, Bioelectrochemistry 101 (2015) 14–21.

[29] Y. Huang, E.Z. Zhou, C.Y. Jiang, R. Jia, S.J. Liu, D.K. Xu, T.Y. Gu, F.H. Wang, Endogenous phenazine-1-carboxamide encoding gene PhzH regulated the extracellular electron transfer in biocorrosion of stainless steel by marine Pseudomonas aeruginosa, Electrochem. Commun. 94 (2018) 9–13.

[30] W.W. Dou, J.L. Liu, W.Z. Cai, D. Wang, R. Jia, S.G. Chen, T.Y. Gu, Electrochemical investigation of increased carbon steel corrosion via extracellular electron transfer by a sulfate reducing bacterium under carbon source starvation, Corros. Sci. 150 (2019) 258–267.

[31] J. Li, Z. Liu, Y. Lou, C. Du, X. Li, Evidencing the uptake of electrons from X80 steel by Bacillus licheniformis with redox probe, 5-cyano-2,3-ditolyl tetrazolium chloride, Corros. Sci. 168 (2020) 108569.

[32] J.o. Philips, N. Van den Driessche, K. De Paepe, A. Prévoteau, J.A. Gralnick, J.B. A. Arends, K. Rabaey, S.-J. Liu, A novel shewanella isolate enhances corrosion by using metallic iron as the electron donor with fumarate as the electron acceptor, Appl. Environ. Microb. 84 (20) (2018).

[33] Z. Li, W. Chang, T. Cui, D. Xu, D. Zhang, Y. Lou, H. Qian, H. Song, A. Mol, F. Cao, T. Gu, X. Li, Adaptive bidirectional extracellular electron transfer during accelerated microbiologically influenced corrosion of stainless steel, Commun. Mater. 2 (2021) 67.

[34] S. Zanna, A. Seyeux, A. Allion-Maurer, P. Marcus, Escherichia coli siderophore-induced modification of passive films on stainless steel, Corros. Sci. 175 (2020) 108872.

[35] Y. Lou, W. Chang, T. Cui, H. Qian, L. Huang, L. Ma, X. Hao, D. Zhang, Microbiologically influenced corrosion inhibition of carbon steel via biomineralization induced by Shewanella putrefaciens, Npj Mat. Degrad. 5 (1) (2021) 59.

[36] N. Guo, Y.N. Wang, X.R. Hui, Q.Y. Zhao, Z.S. Zeng, S. Pan, Z.W. Guo, Y.S. Yin, T. Liu, Marine bacteria inhibit corrosion of steel via synergistic biomineralization, J. Mater. Sci. Technol. 66 (2021) 82–90.

[37] Y.T. Lou, W.W. Chang, T.Y. Cui, J.K. Wang, H.C. Qian, L.W. Ma, X.P. Hao, D. W. Zhang, Microbiologically influenced corrosion inhibition mechanisms in corrosion protection: a review, Bioelectrochemistry 141 (2021) 107833.

[38] T. Liu, Z.W. Guo, Z.S. Zeng, N. Guo, Y.H. Lei, T. Liu, S.B. Sun, X.T. Chang, Y.S. Yin, X.X. Wang, Marine bacteria provide lasting anticorrosion activity for steel via biofilm-induced mineralization, Acs Appl. Mater. Inter. 10 (2018) 40317–40327.

[39] X. Hao, Y. Bai, C. Ren, W. Chang, H. Qian, Y. Lou, L.i. Zhao, D. Zhang, X. Li, Self-healing effect of damaged coatings via biomineralization by Shewanella putrefaciens, Corros. Sci. 196 (2022) 110067.

[40] H.C. Qian, L.W. Ma, D.W. Zhang, Z.Y. Li, L.Y. Huang, Y.T. Lou, C.W. Du, Microbiologically influenced corrosion of 304 stainless steel by halophilic archaea Natronorubrum tibetense, J. Mater. Sci. Technol. 46 (2020) 12–20.

[41] Y. Zhao, E.Z. Zhou, D.K. Xu, Y.G. Yang, Y. Zhao, T. Zhang, T.Y. Gu, K. Yang, F. H. Wang, Laboratory investigation of microbiologically influenced corrosion of 2205 duplex stainless steel by marine Pseudomonas aeruginosa biofilm using electrochemical noise, Corros. Sci. 143 (2018) 281–291.

[42] D. Iravani, R. Arefinia, Effectiveness of one-to-one phosphate to chloride molar ratio at different chloride and hydroxide concentrations for corrosion inhibition of carbon steel, Constr. Build. Mater. 233 (2020) 117200.

[43] H. Li, E. Zhou, D. Zhang, D. Xu, J. Xia, C. Yang, H. Feng, Z. Jiang, X. Li, T. Gu, K. Yang, Microbiologically influenced corrosion of 2707 hyper-duplex stainless steel by marine Pseudomonas aeruginosa biofilm, Sci. Rep.-Uk 6 (1) (2016) 20190.

[44] S. Zhang, Y. Li, Y. Wei, B. Liu, H. Du, H. Wei, L. Hou, Synergistic effect of chloride ions and filmed surface on pitting in the pseudo-passivation behavior of carbon steel, Corros. Sci. 185 (2021) 110042.

[45] Y. Zhao, E.Z. Zhou, Y.Z. Liu, S.J. Liao, Z. Li, D.K. Xu, T. Zhang, T.Y. Gu, Comparison of different electrochemical techniques for continuous monitoring of the microbiologically influenced corrosion of 2205 duplex stainless steel by marine Pseudomonas aeruginosa biofilm, Corros. Sci. 126 (2017) 142–151.

[46] D.-H. Xia, C.-M. Deng, D. Macdonald, S. Jamali, D. Mills, J.-L. Luo, M.G. Strebl, M. Amiri, W. Jin, S. Song, W. Hu, Electrochemical measurements used for assessment of corrosion and protection of metallic materials in the field: a critical review, J. Mater. Sci. Technol. 112 (2022) 151–183.

[47] A.M. Homborg, C.F.L. Morales, T. Tinga, J.H.W. de Wit, J.M.C. Mol, Detection of microbiologically influenced corrosion by electrochemical noise transients, Electrochim. Acta 136 (2014) 223–232.

[48] S. Peng, J. Xu, Z. Li, S. Jiang, Z.-H. Xi, P. Munroe, Electrochemical noise analysis of cavitation erosion corrosion resistance of NbC nanocrystalline coating in a 3.5 wt% NaCl solution, Surf. Coat. Technol. 415 (2021), 127133.

[49] A.M. Homborg, T. Tinga, E.P.M. van Westing, X. Zhang, G.M. Ferrari, J.H.W. de Wit, J.M.C. Mol, A Critical Appraisal of the Interpretation of Electrochemical Noise for Corrosion Studies, Corrosion-Us 70 (2014) 971–987.

[50] C.C. Jiang, G.Y. Xiao, X. Zhang, R.F. Zhu, Y.P. Lu, Formation and corrosion resistance of a phosphate chemical conversion coating on medium carbon low alloy steel, New J. Chem. 40 (2016) 1347–1353.